

Differentially expressed small RNAs in *Arabidopsis* galls formed by *Meloidogyne javanica*: a functional role for miR390 and its TAS3-derived tasiRNAs

Javier Cabrera¹, Marta Barcala¹, Alejandra García¹, Ana Rio-Machín², Clémence Medina³, Stephanie Jaubert-Possamai³, Bruno Favery³, Alexis Maizel⁴, Virginia Ruiz-Ferrer⁵, Carmen Fenoll¹ and Carolina Escobar¹

¹Universidad de Castilla-La Mancha, Facultad de Ciencias Ambientales y Bioquímica, Avda. Carlos III, s/n 45071 Toledo, Spain; ²Molecular Cyrogenetics Group, Human Cancer Genetics Programme, Centro Nacional Investigaciones Oncológicas (CNIO), C/Melchor Fernández Almagro, 3, 28029 Madrid, Spain; ³INRA, Université Nice Sophia Antipolis, CNRS, UMR 1355-7254 Institut Sophia Agrobiotech, 06900 Sophia Antipolis, France; ⁴Centre for Organismal Studies University of Heidelberg, Im Neuenheimer Feld, 230-69120 Heidelberg, Germany; ⁵Centro de Investigaciones Biológicas, CSIC, Av. Ramiro de Maeztu 9, 28040 Madrid, Spain

Author for correspondence:

Carolina Escobar

Tel: +34925268800, ext. 5476

Email: carolina.escobar@uclm.es

Received: 10 August 2015

Accepted: 25 September 2015

New Phytologist (2016) 209: 1625–1640

doi: 10.1111/nph.13735

Key words: galls, giant cells, meloidogyne, miRNAs, rasiRNAs, silencing, small RNAs, tasiRNAs.

Summary

- Root-knot nematodes (RKNs) induce inside the vascular cylinder the giant cells (GCs) embedded in the galls. The distinctive gene repression in early-developing GCs could be facilitated by small RNAs (sRNA) such as miRNAs, and/or epigenetic mechanisms mediated by 24nt-sRNAs, rasiRNAs and 21–22nt-sRNAs. Therefore, the sRNA-population together with the role of the miR390/TAS3/ARFs module were studied during early gall/GC formation.
- Three sRNA libraries from 3-d-post-inoculation (dpi) galls induced by *Meloidogyne javanica* in *Arabidopsis* and three from uninfected root segments were sequenced following Illumina-Solexa technology. *pMIR390a::GUS* and *pTAS3::GUS* lines were assayed for nematode-dependent promoter activation. A sensor line indicative of TAS3-derived tasiRNAs binding to the *ARF3* sequence (*pARF3:ARF3-GUS*) together with a tasiRNA-resistant *ARF3* line (*pARF3:ARF3m-GUS*) were used for functional analysis.
- The sRNA population showed significant differences between galls and controls, with high validation rate and correspondence with their target expression: 21-nt sRNAs corresponding mainly to miRNAs were downregulated, whilst 24-nt-sRNAs from the rasiRNA family were mostly upregulated in galls. The promoters of *MIR390a* and *TAS3*, active in galls, and the *pARF3:ARF3-GUS* line, indicated a role of TAS3-derived-tasiRNAs in galls.
- The regulatory module miR390/TAS3 is necessary for proper gall formation possibly through auxin-responsive factors, and the abundance of 24-nt sRNAs (mostly rasiRNAs) constitutes a gall hallmark.

Introduction

Regulatory small RNAs (sRNAs) are a group of short noncoding RNAs (20–24 nucleotides (nt) long) with diverse roles in gene silencing at the transcriptional and post-transcriptional levels. *Arabidopsis* sRNAs are dominated by short-interfering RNAs (siRNAs) and by microRNAs (miRNAs; Axtell, 2013; Bologna & Voinnet, 2014). Among the endogenous *Arabidopsis* siRNAs there are different sRNAs groups such as trans-acting short-interfering RNAs (ta-siRNAs) and repeat-associated small interfering RNAs (rasiRNAs). Ta-siRNAs are produced through miRNA-guided cleavage of noncoding primary transcripts that are then converted into dsRNA by RDR6, whereas rasiRNAs are generated mostly from transposon loci and DNA repeats. AGO1/7- ta-siRNA complexes mediate the cleavage of mRNA from coding genes, whereas AGO4/6- rasiRNA complexes guide

cytosine methylation in DNA, a landmark of RNA-directed DNA methylation (PolIV-RdDM). Recently, a genetic RdDM pathway was uncovered in *Arabidopsis*. It utilizes 21–22-nt siRNAs as well as 24-nt siRNAs, and methylates ta-siRNAs (Wu *et al.*, 2012; Kanno *et al.*, 2013) and active transposable elements (TEs) by the combined activities of RDR6, DCL2, DCL4 and AGO1 (Nuthikattu *et al.*, 2013). These 21–22-nt siRNAs guide AGO6 to its chromatin targets to establish TE expression-dependent DNA methylation (Wu *et al.*, 2012). Hence, a core of different Dicer-like proteins (DCLs), RNA-dependent RNA polymerases (RDRs) and Argonaute proteins (AGOs) participate in the biogenesis and action of miRNAs, tasiRNAs and rasiRNAs (Axtell, 2013; Bologna & Voinnet, 2014).

In recent years, next-generation sequencing has made clear the importance of sRNA regulation in different abiotic and biotic plant stresses (Sunkar *et al.*, 2012; Balmer & Mauch-

Mani, 2013; Weiberg *et al.*, 2014; Harfouche *et al.*, 2015). Pathogen attack triggers massive miRNA changes, exerting regulatory roles through alteration of hormone pathways, or manipulating silencing pathways to counteract miRNA-mediated defenses, thus regulating plant immunity (reviewed in Balmer & Mauch-Mani, 2013). For example, miR393, implicated in bacterial resistance by repressing auxin signaling, was upregulated in response to the bacterial effector flg22, and targets *TIR1*, *AFB2* and *AFB3* which allow the stabilization of auxin signaling repressor Aux/IAA proteins (Navarro *et al.*, 2006) and viruses use suppressor proteins that interfere with the silencing machinery (Jagga & Gupta, 2014). It can therefore be concluded that miRNAs are very likely to be fundamental players in the concert of broad-spectrum disease resistance (reviewed in Balmer & Mauch-Mani, 2013).

Plant sedentary endoparasitic nematodes are among the most damaging parasites, causing severe agricultural losses (Mitkowski & Abawi, 2003). Two types of sedentary endoparasitic nematodes are described depending on the type of feeding cells that they induce in roots, namely giant cells (GCs) inside galls or knots for root-knot nematodes (RKN; *Meloidogyne* spp; Escobar *et al.*, 2015) and syncytia for cyst nematodes (*Heterodera* spp. and *Globodera* spp.; Bohlmann, 2015). The differentiation of a root vascular cell into a GC or a syncytium, both highly specialized transfer cells, requires dramatic changes in gene expression (reviewed in Escobar *et al.*, 2011, 2015). Generalized gene repression is characteristic of early-developing GCs and galls, and constitutes a signature of early-developing GCs (Schaff *et al.*, 2007; Caillaud *et al.*, 2008; Barcala *et al.*, 2010; Portillo *et al.*, 2013) which includes plant defense-related genes (reviewed in Smant & Jones, 2011; Hewezi & Baum, 2015). For example, peroxidase-coding genes are repressed in compatible interactions, but upregulated in soybean resistant plants (Klink *et al.*, 2009, 2010) and in tomato resistant cultivars homozygous for *Mi-1* (Bar-Or *et al.*, 2005; Schaff *et al.*, 2007). This is consistent with the functional role of tomato TPX1 in resistance to *Meloidogyne javanica* (Portillo *et al.*, 2013). The mechanisms mediating this massive gene repression in early-developing GCs/galls are unknown, but could involve a general differential expression (DE) of sRNAs.

Few massive sequencing experiments have been performed to uncover the role of sRNAs in the plant–nematode interaction and those which have been mainly focused in cyst nematodes (Hewezi *et al.*, 2008; Li *et al.*, 2012; Xu *et al.*, 2014; Zhao *et al.*, 2015). In *Arabidopsis* infected with *Heterodera schachtii*, Hewezi *et al.* (2008) identified 16 miRNAs DE in syncytia at 4 and/or 7 d post inoculation (dpi). Several of them targeted transposons or retrotransposons of different types, suggesting a role for these miRNAs in controlling TE movement (Hewezi *et al.*, 2008; Hewezi & Baum, 2015). *Arabidopsis rdr* and *dcl* mutants altered in essential genes for sRNA biogenesis showed reduced susceptibility to *H. schachtii* (Hewezi *et al.*, 2008). Two sequencing experiments shed light to the sRNA population from resistant and susceptible soybean lines infected with *H. glycines* (Li *et al.*, 2012; Xu *et al.*, 2014), showing several DE miRNAs and siRNAs

between resistant/susceptible plants. A functional role for a miRNA has been demonstrated only for miR396 in *Arabidopsis* syncytia by Hewezi *et al.* (2012). It was shown that miR396 downregulation following *GRF1/GRF3* induction is necessary for correct syncytia initiation. However, subsequent miR396 induction was necessary once the syncytium is established and it does not incorporate new cells. So far, DE sRNAs and their functional roles in RKN feeding sites have not been described, except for systemic stress responses in phloem after RKN inoculation, where the miR319/TCP4 module acts as a systemic signal responder modulating a systemic defensive response mediated by jasmonic acid (Zhao *et al.*, 2015).

Here we analyze the DE sRNAs during early gall development, by using three sRNA libraries from independent biological replicates of hand-dissected 3-dpi galls formed by *M. javanica* in *Arabidopsis*, and uninfected root segments at equivalent positions of the root to obtain three control libraries. We found significant differences between galls and control roots in the sRNA population. In galls, 21-nt sequences corresponding mostly to miRNAs were downregulated, whereas 24-nt sequences from tasiRNAs were upregulated. We studied the expression pattern and functional role of *miR390*, one of the few upregulated miRNAs in galls and GCs at early infection stages. Its promoter is active in GCs and gall vascular tissues and it regulates TAS3-derived tasiRNAs formation in galls. TAS3 was necessary for proper gall development, possibly through the control of auxin-responsive factors. This is the first report of a functional role during plant–nematode interactions of a highly conserved ta-siRNA from bryophytes to vascular plants.

Materials and Methods

Biological materials, growth conditions and nematode inoculation

All *Arabidopsis thaliana* (L.) Heynh lines were in Col-0 background. Seeds were sterilized, and plants grown and inoculated as in Cabrera *et al.* (2014a).

For functional analysis, four independent infection tests were performed for Col-0 (number of plants (*n*) = 280) and *mir390a-2* (*n* = 217), and three independent infection tests with Col-0 (*n* = 114) and *TAS3a-1* (*n* = 114). Gall number per main root was determined under a stereo microscope at 14 dpi. For diameter measurements, at least 21 galls at 14 dpi from three independent experiments were hand dissected, photographed and measured with IMAGEJ (US National Institutes of Health, Bethesda, MD, USA). For significant differences on infection level and gall diameter a Student's *t*-test, *P* < 0.05, was performed using SPSS (IBM, Armonk, NY, USA).

Meloidogyne javanica Treub, 1885 was maintained and *in vitro* infection assays were performed as described in Barcala *et al.* (2010). For *M. incognita*, *Arabidopsis* seeds were stratified in 0.5 × MS/0.8% agar plates at 23°C and 16 h : 8 h, light : dark photoperiod. Twenty days after germination, roots were

inoculated with 200 J2 per plant previously sterilized with 0.01% HgCl₂ and 0.7% streptomycin.

RNA extraction, sRNA library construction and statistical analysis

RNA extractions from three independent samples of *c.* 300 3-dpi galls and three of *c.* 300 control root segments were performed and quality-assessed as in Portillo *et al.* (2009). Each RNA sample extracted from pooled galls or control roots from three or four independent experiments is thus considered a biological replicate. Three of these RNA samples were independently analyzed by massive sequencing for gall or control roots. In each independent experiment, 20 plates containing 10 plants each ($n=200$) were also used to collect galls or control root segments from uninfected plants. Samples were quick-frozen in liquid nitrogen and stored at -80°C .

Illumina-Solexa Sequencing-By-Synthesis technology was used to generate the small-RNA libraries at Beijing Genomics Institute (Shenzhen, China). Clean sequences were obtained after discarding low-quality reads, 5' primer contaminants, and those without 3' primer, without the insert tag, with poly A and/or shorter than 18 nt.

A reads per million (RPM) value was obtained for each sequence in each library (number of reads for a sequence/number of total reads for all sequences in that library $\times 10^6$). Each sequence was tested for expression changes by a two-tailed heteroscedastic *t*-test using statistic software R (R Development Core Team, 2008) between their three independent RPM values in galls and their three independent RPM values in control roots. Expression differences between galls and roots were considered significant when $P < 0.05$. Fold change (FC) was used to measure the expression differences between galls and control roots as the ratio between the average of the RPM values of the three samples in each group. The full raw sequencing data were submitted to the GEO database (<http://www.ncbi.nlm.nih.gov/geo/>) with the accession number: GSE71563.

sRNA sequences annotation

Clean reads were mapped to the Arabidopsis or *M. incognita* genomes (<http://www.arabidopsis.org/> or http://www6.inra.fr/meloidogyne_incognita) by SOAP (Short Oligonucleotide Analysis Package; <http://soap.genomics.org.cn/>) and sRNAs were categorized into types: rRNA, tRNA and snRNA were analyzed in GenBank and in RFAM; known miRNAs and their isomiRs (miRBase19), repeats, exon and intron were analyzed by BGI Genomics in-house database.

Unannotated sequences were screened with Mireap (<http://sourceforge.net/projects/mireap/>) which predicts novel miRNA by exploring secondary structure, DICER cleavage site and minimum free energy (MFE) of the unannotated small RNA tags. The following restrictions were imposed: minimal miRNA sequence length (18 nt), maximal miRNA sequence length (25 nt), minimal miRNA reference sequence length (20 nt), maximal miRNA reference sequence length (23 nt),

maximal copy number of miRNAs on reference (20 nt), maximal free energy allowed for a miRNA precursor ($-18 \text{ kcal mol}^{-1}$), maximal space between miRNA and miRNA* (300 nt), minimal base pairs of miRNA and miRNA* (16 nt), maximal bulge of miRNA and miRNA* (4 nt), and maximal asymmetry of miRNA/miRNA* duplex (4 nt).

Target prediction was performed on the Plant Small RNA Target Analysis Server (psRNATarget; <http://plantgrn.noble.org/psRNATarget/>; Dai & Zhao, 2011). The following restrictions were established: maximum expectation (3.0), length for complementarity scoring (20), allowed maximum energy to unpair the target site (UPE; 25); flanking length around target site for target accessibility analysis (17 bp in upstream/13 bp in downstream); and range of central mismatch leading to translational inhibition (9–11 nt).

q-PCR validation of the expression of miRNAs and their targets, histological analysis of GUS expression and gall phenotyping

Expression levels of selected miRNAs DE in the libraries were analyzed by qRT-PCR using TaqMan[®] Small RNA assays. The probes used were: aly-miR156 h (463816_mat), miR163 (343), miR167d (000350), miR390a (001409miR775 (008366_mat), miR780.2 (464297_mat), miR839 (008535_mat) and aly-miR857 (006362_mat). qRT-PCR was performed as described by Frenquelli *et al.* (2010)). The independent RNA samples used for RNAseq were used for cDNA synthesis. Total RNA (10 ng) was reverse-transcribed with the MicroRNA Reverse Transcription Kit (Applied Biosystems, Foster City, CA, USA) in a final reaction volume of 5 μl . Independent reverse transcription reactions were set for each miR-snoR pair. qRT-PCR was performed using TaqMan Fast Universal PCR Master Mix on a 7500 Fast Real-Time PCR System following the manufacturer's protocol. Each independent cDNA template was run in triplicate (384-well plate). Data were normalized to the expression of two small nucleolar RNAs (predesigned TaqMan[®] small RNA control assays snoR101 and snoR66; Applied Biosystems) and relative expression was calculated using the comparative Ct method ($2^{-\Delta\Delta\text{Ct}}$). Tendencies were similar with both normalizers.

Validation of the transcript level for predicted miRNA target genes was performed by qRT-PCR. RNA samples used for sequencing were reverse transcribed with the High-Capacity cDNA Reverse Kit (Applied Biosystems), using 500 ng of RNA per reaction and following manufacturer's instructions. Normalization was referred to *GAPC2* according to the method of Barcala *et al.* (2010). Relative expression was calculated using the comparative Ct method ($2^{-\Delta\Delta\text{Ct}}$). Primer sequences are listed in Supporting Information Table S1.

For all q-PCR data a Student's *t*-test was performed ($P < 0.05$) to identify FC differences between galls and uninfected controls.

For tissue localization of GUS activity, seedlings from *pMIR390a::GUS*, *pTAS3::GUS*, *pARF3:ARF3-GUS* and *pARF3:ARF3 m-GUS* lines were treated and phenotyped as described in Cabrera *et al.* (2014a).

Results

Overview of sRNAs expressed in galls and control roots

Illumina-Solexa Sequencing-By-Synthesis technology was used to generate three independent sRNA libraries from *c.* 300 hand-collected 3-dpi galls each, and three libraries from their corresponding control roots (see the Materials and Methods section; Fig. 1a). An average of 10.1 million raw reads (Solexa 50 nt reads) were obtained for the three gall libraries (G1, G2 and G3), and an average of 9.8 million for control roots (R1, R2, R3) (Fig. 1b). After filtering reads, the number of clean reads was reduced to an average of 9.8 million for galls and 9.5 million for control roots (Fig. 1b). The similar overall numbers obtained for the three libraries in both sample types indicate a high uniformity among the three biological replicates used for the analysis. An average of 2121 427 clean reads corresponded to unique sRNA sequences in the three gall libraries, almost twice the 1241 364 reads obtained for the control root libraries (Fig. 1b). In the six libraries, 99.9% of the reads had a length between 18 and 29 nt

(Fig. 2a), most of them ranging from 20 to 24 nt, the typical length of small RNAs processed by DICER (Ghildiyal & Zamore, 2009). Read-length distribution in each library was similar except for the 24-nt sequences, which were consistently more abundant in gall than in control root libraries (Fig. 2a). By contrast, 20- and 21-nt reads (the typical length of miRNAs; Ghildiyal & Zamore, 2009) were consistently larger in root than in gall libraries (Fig. 2a). Fifty-eight percent of the unique sRNA sequences in the six libraries were present exclusively in galls, whilst only 16.2% were exclusive from control roots and 25.8% were shared between both (Fig. 2b). The matched sequences were aligned against sequences in GenBank, Rfam and miRBase to find previously known sRNAs. Fig. 2(c) summarizes the number of sequences found in each library corresponding to different sRNA types. Approximately half of the unique sequences (54% and 50% for galls and control roots, respectively) were unannotated; that is, either they could not be mapped to the Arabidopsis genome (and could be of nematode origin) or they hit Arabidopsis sequences not classified as sRNAs (Fig. 2c).

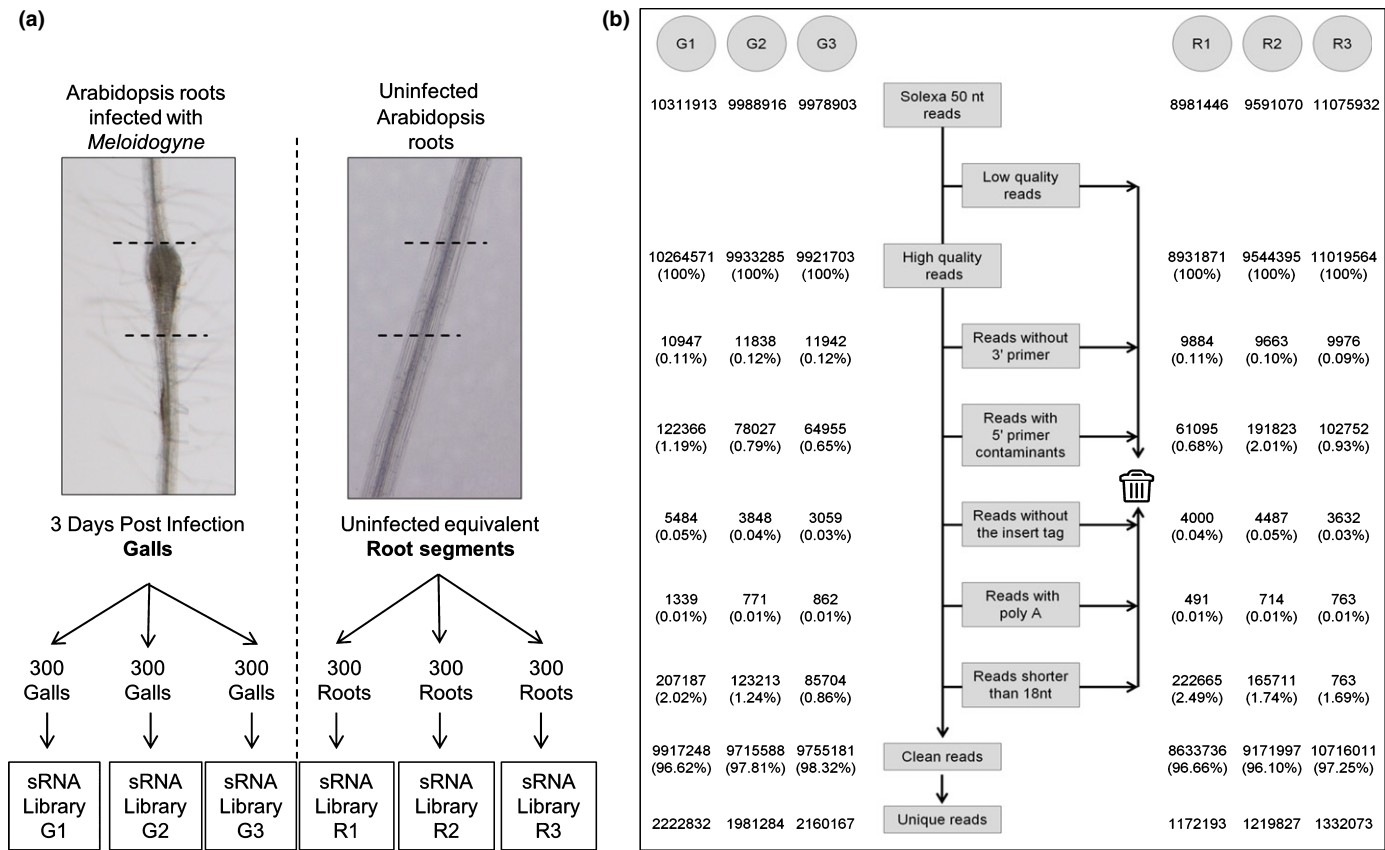


Fig. 1 Schematic representation of sRNA library construction and clean read generation. (a) Approximately 900 at 3-d-post-infection (dpi)-galls induced by *Meloidogyne javanica* in *Arabidopsis thaliana* were collected in three independent biological replicates (left panel) for construction of gall libraries (G1, G2 and G3). Equivalent root segments from uninfected plants grown in the same conditions were collected also in triplicate for uninfected root libraries (R1, R2 and R3; right panel). Dotted lines in the pictures indicate the hand-dissected segments collected. (b) Number of discarded or retained reads is indicated in each step, as well as the percentage that this number represents with respect to the total number of high-quality reads for each library. Clean reads are obtained after discarding reads without 3' primers, with 5' primers contaminants, without the insert tag, with poly A, or shorter than 18 nt, and low-quality sequences. Unique reads represent those distinct sequences read.

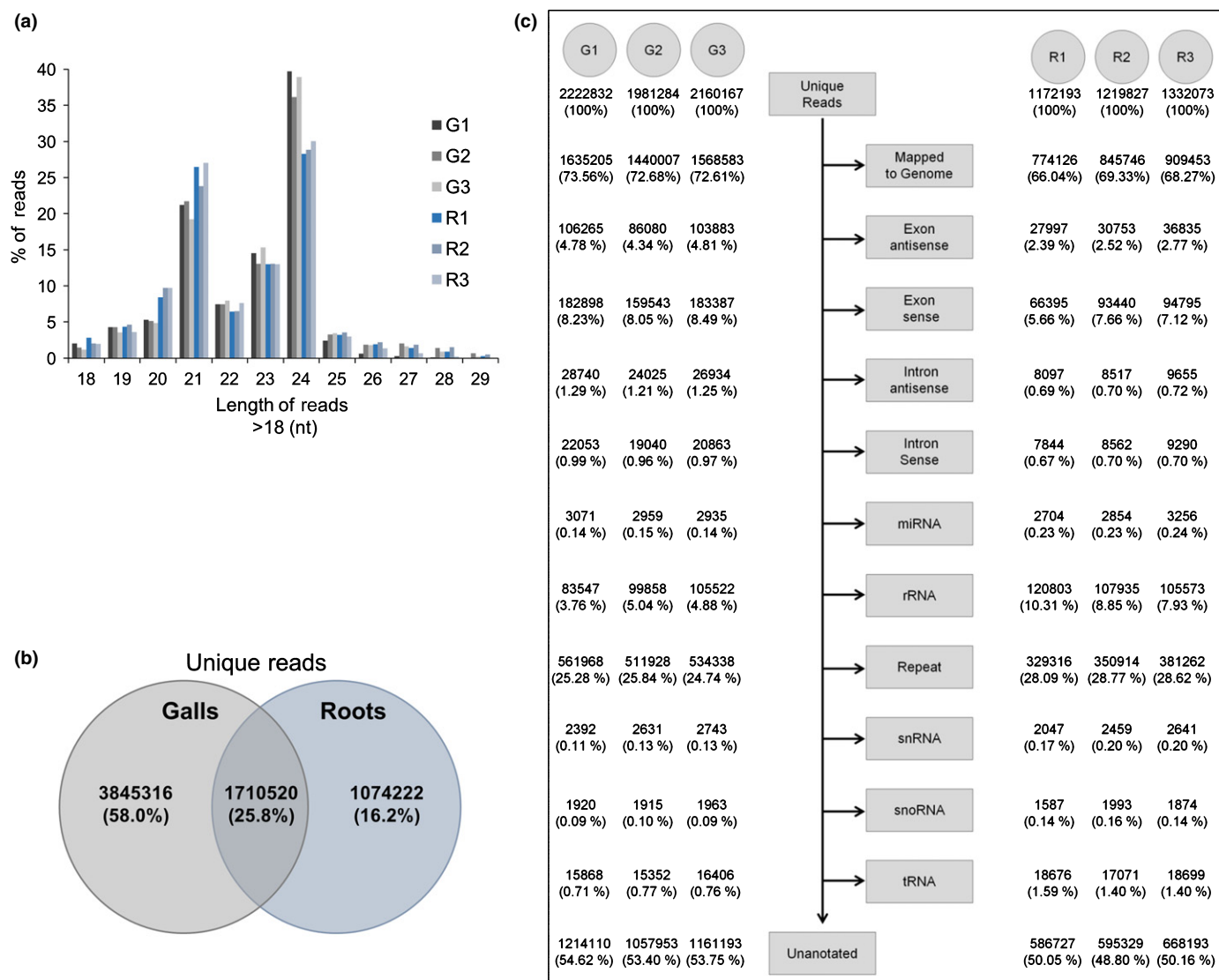


Fig. 2 General sRNA analysis in galls induced by *Meloidogyne javanica* in *Arabidopsis thaliana* and control libraries. (a) Distribution of clean reads (in %) in the six libraries catalogued into length categories. Note the marked abundance of the 24-nt sequences in gall libraries, with an average of 3803 611 sequences as compared to the 2826 085 found in libraries from control roots. (b) Venn diagram indicating number and percentage of unique reads exclusive and/or shared by galls and control roots libraries. (c) Schematic representation of the annotation process of the reads by alignment to the genome and adscription to different small RNA categories (miRNA, rRNA, tRNA, snRNA, snoRNA, repeat, exon, intron). Note that the abundance of intron and exon antisense sequences is higher in galls than in control libraries.

Differential expression of sRNAs and identification of their putative targets in the *Arabidopsis* genome

From the 338 known *Arabidopsis* miRNAs, 288 were detected in at least one library, whereas 50 were not identified in any read through the six libraries (Table S2). The overall numbers of reads for each miRNA among the libraries from either galls or control roots presented similar trends (Table S2), reinforcing the validity of the sequencing in the three biological replicates. From the 265 different miRNAs identified in each library, 242 were common to both conditions, 23 were exclusive of galls and 23 were only present in control root libraries (Table S2). For simplicity, the terms differentially expressed (DE), induced/

upregulated and repressed/downregulated are used throughout the text to mean mature sRNA levels higher or lower than in their corresponding controls, respectively. Interestingly, the average number of reads corresponding to known miRNAs in the three control root libraries (24 227) was 1.7-fold that of the three gall libraries (14 617), suggesting a global downregulation of miRNA in galls (Table S2). Accordingly, after normalization of the reads as 'reads per million' and analysis of DE miRNAs (see the Materials and Methods section), only 11 of the 288 miRNAs detected were upregulated ($P < 0.05$), whereas 51 were downregulated in galls ($P < 0.05$; Table 1). From the 62 DE miRNAs, large miRNA families as miR166 and miR169 were consistently downregulated in galls (Table 1). By

Table 1 Average number of reads for known miRNAs in gall and control root libraries

	Average no. of reads		FC	P-value
	Gall libraries	Root libraries		
ath-miR156i	5	1	7.06	0.032
ath-miR839	19	5	3.74	0.028
ath-miR5657	64	18	3.47	0.017
ath-miR851-3p	10	3	2.94	0.016
ath-miR390a	53 602	19 921	2.70	0.007
ath-miR390b	53 586	19 917	2.70	0.007
ath-miR391	42	16	2.62	0.002
ath-miR5655	113	45	2.46	0.042
ath-miR775	790	368	2.13	0.012
ath-miR156h	1478	720	2.02	0.020
ath-miR5643a	58	38	1.50	0.047
ath-miR159b	312	459	-1.52	0.049
ath-miR166a	127 138	191 088	-1.54	0.027
ath-miR166g	121 322	182 951	-1.55	0.025
ath-miR166c	121 384	183 056	-1.55	0.025
ath-miR166e	121 289	182 914	-1.55	0.025
ath-miR166d	121 384	183 059	-1.55	0.025
ath-miR166f	121 284	182 909	-1.55	0.025
ath-miR166b	121 344	183 020	-1.55	0.025
ath-miR5645f	113	176	-1.59	0.044
ath-miR5645e	112	174	-1.59	0.036
ath-miR5645a	112	176	-1.60	0.037
ath-miR5645b	112	176	-1.60	0.037
ath-miR165a	40 918	65 318	-1.65	0.044
ath-miR165b	39 533	63 672	-1.67	0.044
ath-miR5635a	75	130	-1.78	0.011
ath-miR5635d	260	503	-1.98	0.005
ath-miR156j	431	1009	-2.40	0.010
ath-miR156b	191 210	461 888	-2.47	0.013
ath-miR156a	191 007	461 738	-2.47	0.013
ath-miR156c	191 007	461 738	-2.47	0.013
ath-miR156e	190 500	461 235	-2.48	0.013
ath-miR156f	190 497	461 238	-2.48	0.013
ath-miR156d	192 256	470 427	-2.50	0.014
ath-miR5653	448	1102	-2.54	0.001
ath-miR399e	5	15	-3.02	0.028
ath-miR156g	187	569	-3.13	0.000
ath-miR169f	41	129	-3.30	0.004
ath-miR857	3	8	-3.30	0.032
ath-miR169j	20	70	-3.53	0.023
ath-miR169n	20	70	-3.53	0.023
ath-miR169l	20	70	-3.55	0.026
ath-miR169g-5p	37	128	-3.55	0.004
ath-miR163	56	200	-3.66	0.015
ath-miR169i	20	72	-3.67	0.021
ath-miR169h	6	21	-3.79	0.023
ath-miR169k	6	21	-3.79	0.023
ath-miR167d	67	263	-3.99	0.041
ath-miR169d	33	126	-4.01	0.004
ath-miR169e	33	126	-4.01	0.004
ath-miR169m	6	23	-4.03	0.024
ath-miR5644	26	102	-4.09	0.029
ath-miR399b	11	46	-4.12	0.003
ath-miR172b-3p	108	482	-4.53	0.029
ath-miR172a	108	483	-4.54	0.028
ath-miR319b	6	27	-4.88	0.003
ath-miR780.2	4	21	-5.45	0.003
ath-miR5648-3p	8	70	-8.58	0.034
ath-miR2111a-5p	2	21	-10.82	0.001

Table 1 (Continued)

	Average no. of reads		FC	P-value
	Gall libraries	Root libraries		
ath-miR2111b-5p	2	21	-10.82	0.001
ath-miR5637	0	4	-12.40	0.001
ath-miR172e	2	35	-17.67	0.000

The three libraries for galls induced by *Meloidogyne javanica* in *Arabidopsis thaliana* and roots are represented separately. Fold change (FC) and statistical significance (*P*-value) for the differentially expressed miRNAs are indicated. Red, induced, and green, repressed miRNAs in galls tested by q-PCR in Fig. 3(a).

contrast, miR390a and miR390b were highly upregulated (FC = 2.70) in galls (Table 1) as were two members of the miR156 family (miR156 h-i; FC = 7.06; Table 1), although the majority of the members of this family were downregulated (miR156a-g, j).

Fold change values for the DE miRNAs were validated by TaqMan[®] assay-based real-time PCR (Fig. 3a). Seven miRNAs were selected for validation, three induced and four repressed in galls, representative of different expression patterns in both libraries; that is, a high number of readings (e.g. miR390a), low number of readings (e.g. miR857), and intermediate number of readings (e.g. miR775s). qPCR was done after cDNA synthesis with the same RNA samples used for the construction of the six small RNA libraries, and resulted in a high validation rate of the sequencing results (6 out of 7 tested; Fig. 3a). Different sensitivities of both techniques might explain the nonvalidated expression pattern of miR167d.

The potential target genes of the known DE miRNAs were downloaded from the Plant MicroRNA Database (<http://bioinformatics.cau.edu.cn/PMRD/>; Zhang *et al.*, 2010) and were also predicted by using the psRNATarget web server (<http://plantgrn.noble.org/psRNATarget/>) accomplishing restrictive parameters (see the Materials and Methods section). The TAIR10 transcripts database was used as the reference genome, identifying 108 putative target genes for the upregulated and 222 for the downregulated miRNAs in galls, respectively (Table S3). Some of the predicted targets had been experimentally validated in different biological systems, for example, those for miR390, miR156 or miR172 that preferentially target TAS3, trans-acting short-interfering RNA 3 (Montgomery *et al.*, 2008), SQUAMOSA PROMOTER BINDING PROTEINS (*SPLs*; Wu & Poethig, 2006) and R-homologous Arabidopsis protein (RAP) (Aukerman & Sakai, 2003), respectively. Classification into functional categories with Mapman (Thimm *et al.*, 2004) determined that most targets belong to the category of 'Regulation of Transcription', particularly to the transcription factors subcategory, with 35 transcription factors among the putative targets of downregulated miRNAs and 8 among the targets of the upregulated miRNAs in galls (Table S3). It is also important to point out the identification of 26 transposable elements (TEs) as putative targets of the DE miRNAs (Table S3).

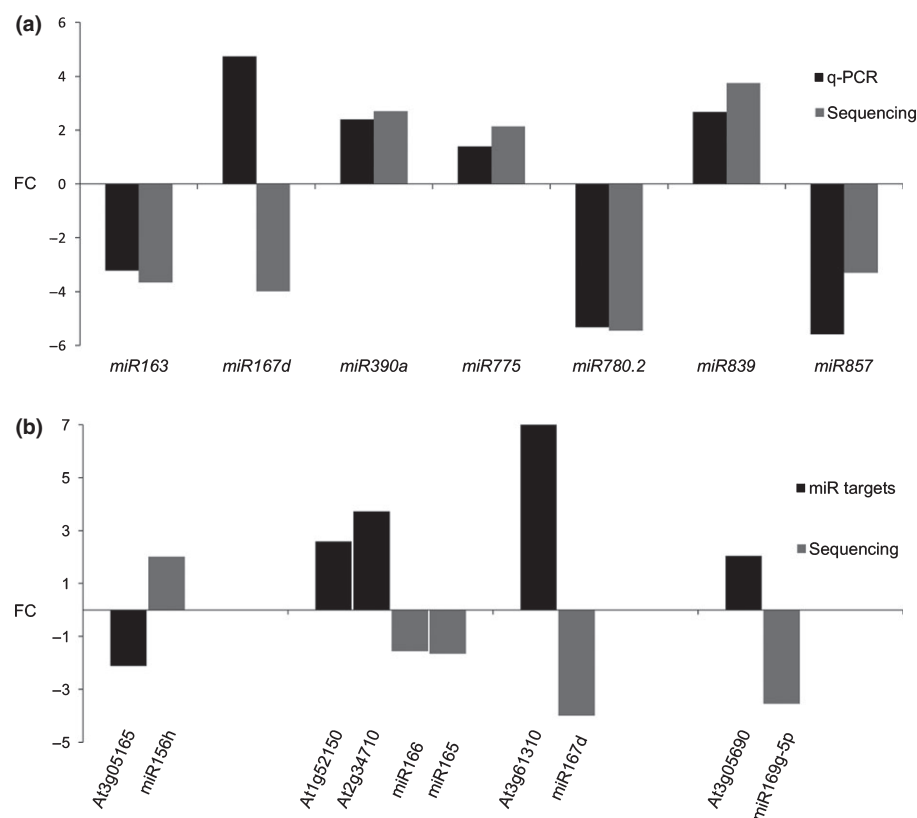


Fig. 3 Quantitative-PCR (q-PCR) analysis of differentially expressed miRNAs and their predicted targets in galls induced by *Meloidogyne javanica* in *Arabidopsis thaliana*. (a) miRNA expression values in galls relative to uninfected controls by RNAseq (gray) and q-PCR (black). All miRNAs tested showed significant expression differences between galls and controls ($P < 0.05$) by RNA-seq and q-PCR, except miR839 by q-PCR with $P < 0.16$. (b) Expression of six putative miRNA targets measured by q-PCR. All were repressed in galls vs control roots ($P < 0.05$) agreeing with microarray data (Jammes *et al.*, 2005; Barcala *et al.*, 2010). FC, fold change.

A role for miR390 during root-knot nematode infection

miR390a-b were highly expressed in galls, showing the highest number of readings among those up-regulated miRNAs described (*c.* 53 000 each; Table 1). As *MIR390a* (At2g38325) is also predominantly expressed in roots (Marin *et al.*, 2010), we analyzed its promoter activation pattern during nematode infection. A GUS reporter line carrying a 2.6-kb promoter region from *MIR390a* (Fig. 4a–c; Marin *et al.*, 2010) was specifically activated within 4-dpi galls (Fig. 4a) induced by *M. javanica* in *Arabidopsis* roots, whereas in uninfected roots it was only detected in lateral root primordia and in the elongation zone (Fig. S1a,b). Hence, *pMIR390a::GUS* activation pattern was consistent with our sequencing and q-PCR results (Table 1; Fig. 3a). GUS activity in galls was maximal at 7 dpi (Fig. 4b) and decreased at medium-late infection stages (15 dpi; Fig. 4c). GUS activity was localized in the GCs and surrounding cells within the vascular cylinder in semi-thin 4-dpi gall sections (Fig. 4g). The expression pattern of *pMIR390a::GUS* was similar in 5- and 7-dpi galls induced by the related species *M. incognita* (Fig. S1e, f).

We then investigated its functional role during gall development. The homozygous line *mir390a-2*, carrying a T-DNA insertion located 30 bp upstream of the *MIR390a* (At2g38325) transcription start site, showed a strong reduction in the accumulation of the mature miR390a in roots, compared to the wild-type line (Marin *et al.*, 2010) and is therefore considered a loss-of-function line. When tested for nematode infection, this line presented a significant decrease ($P < 0.05$) in infection levels (23% less galls per main root than the wild-type Col-0 line;

Fig. 5a). Moreover, galls formed in the *mir390a-2* line were smaller than those formed in Col-0 plants ($P < 0.05$; Fig. 5b). This suggests that miR390a expression in galls is important for successful nematode infection.

In roots, miR390 controls the biogenesis of *TAS3* derived trans-acting short-interfering RNAs (tasiRNAs), and this function is crucial for lateral root growth (Marin *et al.*, 2010). The *pTAS3a::GUS* line showed activation along the vascular tissue of uninfected roots and in *M. javanica*-induced galls (Fig. S1c,d; Fig. 4d–f). The activation observed at 4 dpi was maintained in 7- and 15-dpi galls (Fig. 4d–f). In semi-thin sections of 4 dpi galls, the GUS signal was intense in GCs as well as in their neighboring cells (Fig. 4h). Thus, the expression patterns of *pTAS3a::GUS* and *pMIR390a::GUS* overlap in galls, similarly to those described for lateral roots (Marin *et al.*, 2010). *TAS3a* role in galls was analyzed by performing infection tests in the mutant line *TAS3a-1* (GABI 621G08), with only 40% of wild-type *TAS3a* transcript levels; Marin *et al.*, 2010). This mutant line presented a 40% reduction in the percentage of galls per main root with respect to the control (Fig. 5c). The galls formed in *TAS3a-1* were not significantly different in size to those of the control (Fig. 5d). It has been demonstrated that miR390a, *TAS3*-derived tasiRNAs and the auxin responsive factors ARF2, ARF3 and ARF4, constitute an auxin-responsive regulatory module controlling lateral root growth, in such a way that active *TAS3*-derived tasiRNAs regulate these ARFs directly in lateral roots by degrading their transcripts (Marin *et al.*, 2010). Accordingly, a GUS-based sensor line that is not induced when the *TAS3*-derived tasiRNAs are actively binding the ARF3 sequence, *pARF3:ARF3-GUS*, was not induced in

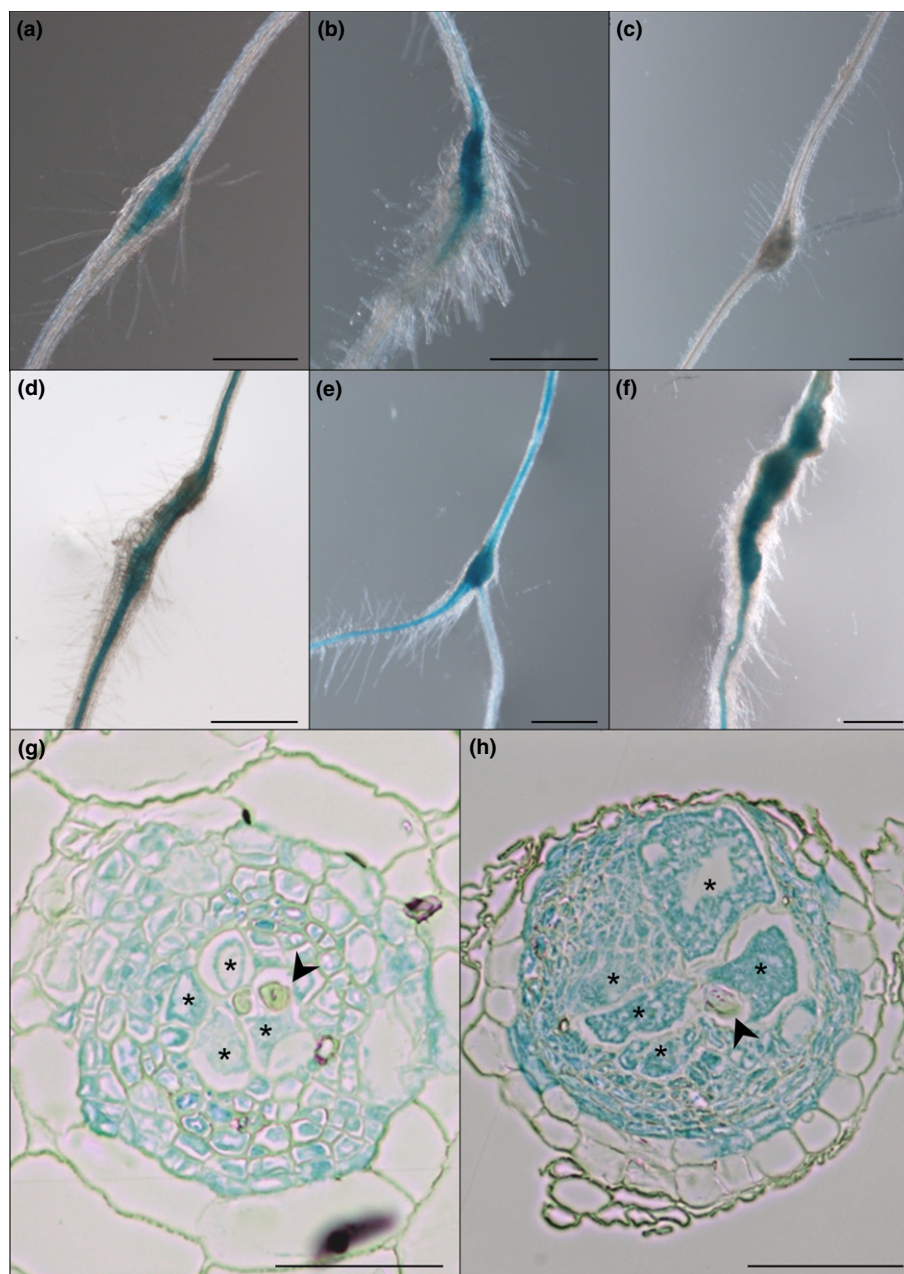


Fig. 4 Overlapping expression patterns of *pMIR390a::GUS* and *pTAS3::GUS* in galls. *pMIR390a::GUS* is active in galls induced by *Meloidogyne javanica* in Arabidopsis at 4 d post infection (dpi) (a), reaching its maximum expression at 7 dpi (b). Expression disappears at 15 dpi (c). *pTAS3::GUS* is activated in the vascular cylinder and inside galls at 4 dpi (d). Its expression is maintained at 7 (e) and 15 (f) dpi. GUS signal was localized in giant cells (GCs) and surrounding cells in the vascular cylinder in semi-thin sections of 4-dpi galls from *pMIR390a::GUS* (g) and *pTAS3::GUS* (h). Asterisks indicate GCs. Black arrowhead indicates nematode. Bars: (a–f) 500 μ m; (g, h) 100 μ m.

galls (Fig. 6a). By contrast, a line harboring an *ARF3* sequence resistant to the cleavage by *TAS3*-derived *tasiRNAs* (*pARF3::ARF3m-GUS*; induced in the tissues where the promoter is active) was activated in galls at 3 dpi (Fig. 6b). GUS staining in this line showed the same pattern in GCs and surrounding cells as the *MIR390a* promoter and the *TAS3a* promoter lines (Figs 4g,h, 7c). These results confirmed that *TAS3*-derived *tasiRNAs* were active in galls and GCs, as they could degrade their described mRNA target, *ARF3*.

Identification of putative nematode-responsive novel miRNAs

Those sRNA sequences that mapped in the Arabidopsis genome but were not classified as any previously described miRNA were

analyzed using Mireap software (<http://sourceforge.net/projects/mireap/>) to predict their secondary structures, *DICER* cleavage sites and MFE (minimum free energy; $-40/-74$ kcal mol $^{-1}$; Bonnet *et al.*, 2004). Six hundred and two sequences ranging from 19 to 25 nt and present in at least one of the six libraries presented structural hairpin characteristics. However, only 11 of these sequences ranging from 21 to 23 nt were DE ($P < 0.05$) in galls as compared to control roots, three of them being upregulated and eight downregulated (Table 2). From them, one upregulated and two downregulated also presented MFE values similar to those described for Arabidopsis miRNAs (Table 2). Interestingly, one was exclusively read in control root libraries, another one only in galls, and another sequence was abundant in both, although upregulated in galls (Table 2). The potential targets for these three putative sRNAs were predicted, finding among them

Fig. 5 The role of miRNA390 and TAS3 during the infection of *Arabidopsis thaliana* by *Meloidogyne javanica*. Mutant lines infected with *Meloidogyne javanica* showed a significant decrease in the infection rate. A 23% decrease in the infection level was observed for the mutant *mir390a-2* line (a), as well as a reduction in the size of the formed galls (b). *TAS3a-1* mutant line presented a significant reduction of 40% in the percentage of galls per main root with respect to the Col-0 control (c), but galls were not smaller than those of the control (d). Statistical analysis was performed with three independent experiments per line using ANOVA; significant differences with Col-0 are indicated by asterisks, $P < 0.05$; values are means \pm SE.

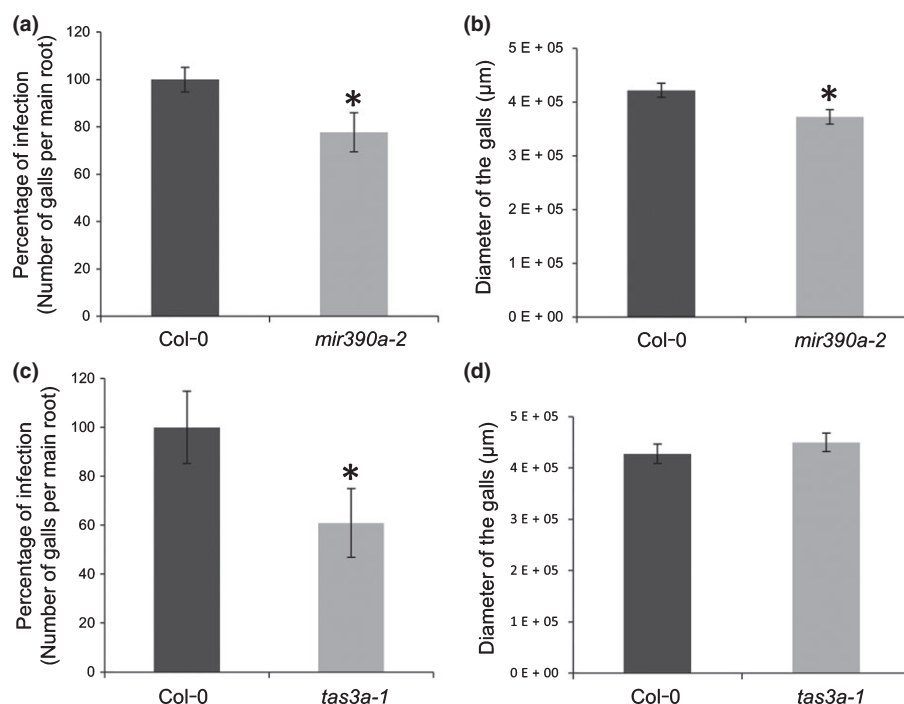
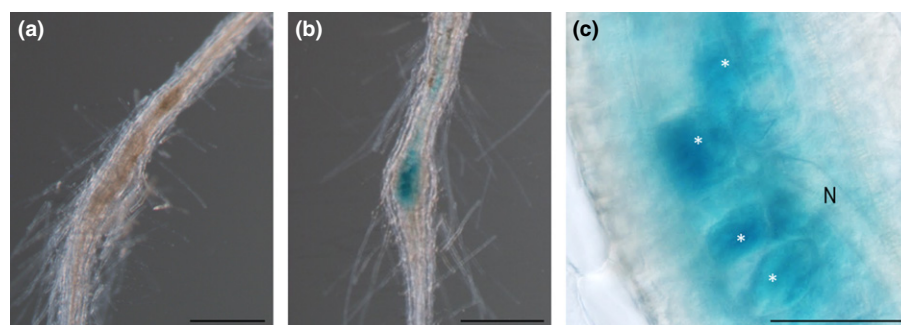


Fig. 6 *TAS3*-derived *tasiRNAs* are active in galls and giant cells (GCs) as they could degrade *ARF3*. At 3 d post infection (dpi), *pARF3:ARF3-GUS* is not induced in galls induced by *Meloidogyne javanica* in *Arabidopsis thaliana* (a), whereas *pARF3:ARF3m-GUS*, a mutated version resistant to *TAS3*, is activated in galls (b), and giant cells (c). Asterisks indicate giant cells. N, nematode. Bars: (a, b) 500 μm; (c) 100 μm.



genes related to stress, hormone metabolism, development or cell cycle (Table S4).

Comparative expression analysis of miRNAs and their targets

The expression of the predicted targets for the upregulated miRNAs in 3-dpi galls (Tables 3, S3) was checked among downregulated genes identified in previous studies, and vice versa. The transcriptomes used were from 3-dpi microdissected GCs and galls (Barcala *et al.*, 2010), and 7 dpi-galls (Jammes *et al.*, 2005; Cabrera *et al.*, 2014b). In these comparisons, six downregulated genes ($P < 0.05$) were predicted as putative targets of six upregulated miRNAs described in this work (Table 3). We found 15 upregulated transcripts that were putative targets of downregulated known and novel miRNAs in our analysis (Table 3). Among them is *MYB33* (targeted by miR159b and miR319b), the only MYB transcription factor upregulated in 3-dpi GCs (Barcala *et al.*, 2010).

A double validation of some of these putative targets by q-PCR showed the same tendencies as in microarray analysis (Fig. 3b; Barcala *et al.*, 2010; Jammes *et al.*, 2005). The selected miRNAs and the mRNA abundance of their predicted targets showed opposite behavior as expected.

Overview and differential expression of 24-nt sRNAs and rasiRNAs

The length distribution overview of the sequences found in the six libraries showed a marked increase in the number of 24-nt reads in galls compared to control roots (Fig. 2a). To investigate the importance of this group of 24-nt sRNAs in galls, a DE analysis was performed after normalization of reads as RPM. From the 2909 193 unique 24-nt sequences found in at least one of the six libraries, 1.94% (corresponding to 56 455 sequences) were DE statistically (Fig. S2). From those, 35% (19 970) were expressed exclusively in galls, whereas 2557 (4.5%) were exclusive from control roots (Fig. S2). From the 33 928 sequences shared

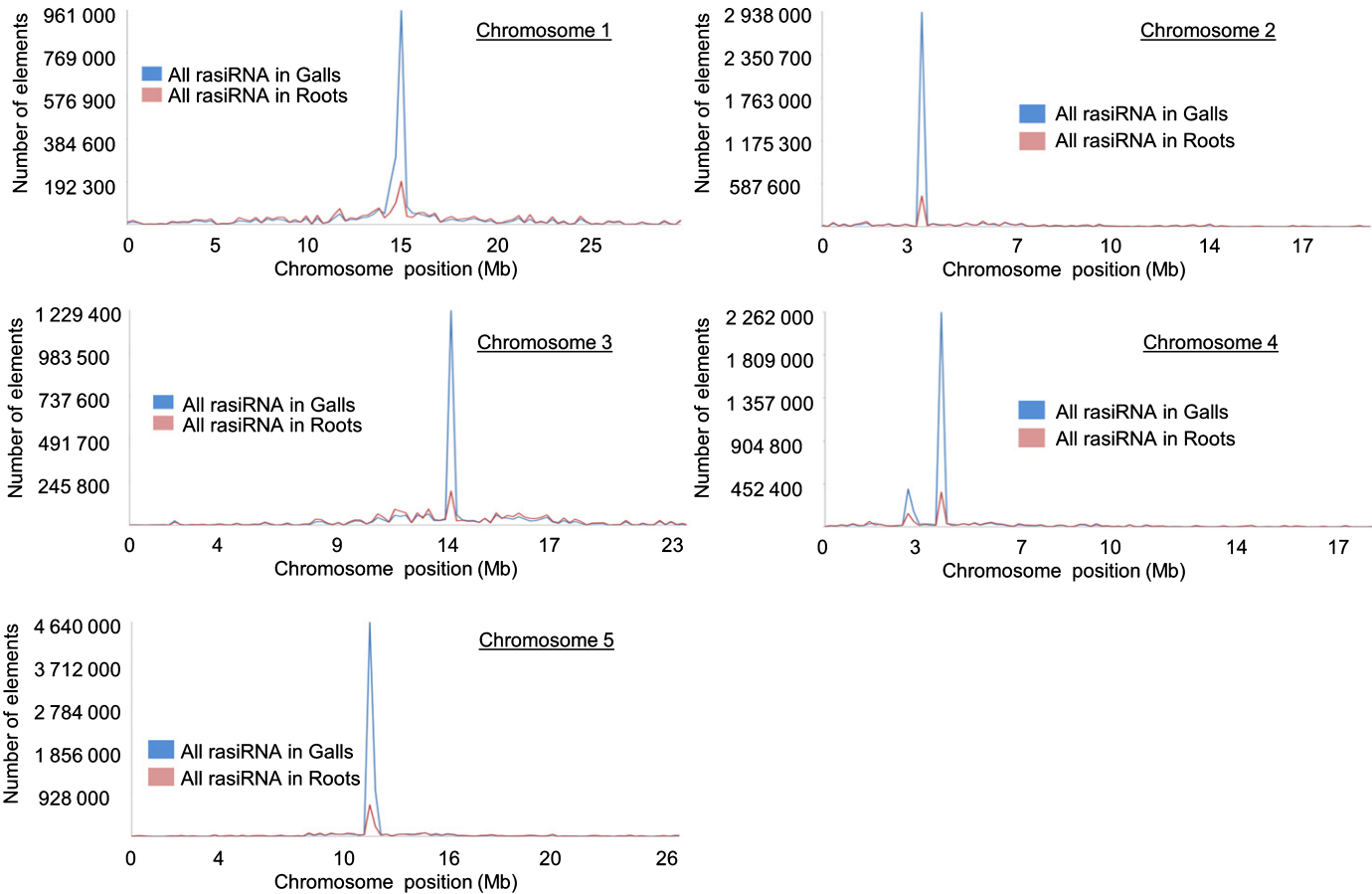


Fig. 7 Distribution of rasiRNAs from *Meloidogyne javanica* galls and control roots in the Arabidopsis genome. Repeat-associated small interfering RNAs in gall and control libraries are shown across the five Arabidopsis chromosomes. x-Axis indicates chromosome position and y-axis the number of reads.

Table 2 Novel Arabidopsis miRNAs identified in galls induced by *Meloidogyne javanica* and control root libraries

	Length	Minimum Free Energy	Total number of Reads						P value
			G1	G2	G3	C1	C2	C3	
GAAGGTAGAGTTGTAGAGAGGTT	23	−61.3	16	11	10	0	0	0	0.020
AGAGAGAGAGAGAGAAGAGCAA	22	−28.2	11	5	8	0	0	0	0.042
TTGAGGGGGGTGTATTAATAATA	23	−24	9	14	15	0	0	0	0.022
GAAAGGAATTTGCGGTAGATATA	23	−73.2	1515	1622	1813	1988	2356	2643	0.004
GGGGGCTTTTGAAGAATTGGCAC	23	−31.6	28	0	40	72	62	83	0.035
TGATGAAC TCGCAATTAGACGTA	23	−36.9	0	0	0	10	13	12	0.006
TGGATAGAGATGAGTGATGGATA	23	−22.3	0	0	0	970	1409	1331	0.009
GGAATGATGAGGAAAAATGTA	21	−18	0	0	0	15	13	15	0.005
GTGGAAGAAAGAGAAGATGATA	22	−47.2	0	0	0	17	19	24	0.001
GGTCATGATCGCGGTCACGGT	21	−69.1	0	0	0	17	13	19	0.009
ATGGAAGAGTGATATGGATAA	21	−44.4	0	0	0	40	70	64	0.020

The length, minimum free energy, total number of reads in the six libraries and statistical significance (P-value) for the differentially expressed novel miRNAs identified in galls and control roots are indicated. In bold those sequences with a minimum free energy suitable for miRNAs.

by galls and controls, 67.7% (22 974) were upregulated in galls, whereas only 10 954 were repressed (Fig. S2). Therefore, from the 56 455 sequences of 24-nt DE, 42 944 (76%) were either exclusive or upregulated in galls (Fig. S2). Strikingly, up to 1537 sequences of 24 nt presented a FC higher than +20, showing

remarkable differences in their expression levels in galls as compared to the control roots. Comparison of these results to those relative to the sRNAs of 20–21 nt described above, mostly down-regulated in galls, indicate a contrasted regulation between 20–21-nt sRNAs and 24-nt sRNAs in galls.

Table 3 Predicted targets of differentially expressed (DE) miRNAs

miRNA	Target ID	Description
ath-miR156h	AT3G05165	sugar transporter, putative
ath-miR156i	AT2G17220	Protein kinase superfamily protein
ath-miR5643a	AT1G45130	BGAL5 beta-galactosidase 5
ath-miR5655	AT4G28270	ATRMA2, RMA2 RING membrane-anchor 2
ath-miR5657	AT1G20950	Phosphofructokinase family protein
NewSeq1	AT5G51690	ACS12 1-amino-cyclopropane-1-carboxylate synthase 12
ath-miR156a,b,c,d,e,f,g,j	AT5G50670	squamosa promoter-binding protein, putative
ath-miR156j	AT5G08620	STRS2, ATRH25 STRS2 (STRESS RESPONSE SUPPRESSOR 2)
ath-miR159b/ath-miR319b	AT5G06100	MYB33, ATMYB33 MYB33 (MYB DOMAIN PROTEIN 33); DNA binding/transcription factor
ath-miR163	AT3G44870	S-adenosyl-L-methionine:carboxyl methyltransferase family protein
ath-miR163	AT5G37990	S-adenosyl-L-methionine-dependent methyltransferases superfamily protein
ath-miR165a,b/ath-miR166a,b,c,d,e,f,g	AT2G34710	PHB, ATHB14, ATHB-14, PHB-1D PHB (PHABULOSA); DNA binding/transcription factor
ath-miR165a,b/ath-miR166a,b,c,d,e,f,g	AT1G52150	ATHB-15, ATHB15, CNA, ICU4 ATHB-15; DNA binding/transcription factor
ath-miR167d	AT3G61310	DNA-binding family protein
ath-miR169d,e,f,g,h,i,j,k,l,m,n	AT5G06510	NF-YA10 NF-YA10 (NUCLEAR FACTOR Y, SUBUNIT A10); transcription factor
ath-miR169d,e,f,g,h,i,j,k,l,m,n	AT3G05690	NF-YA2 (NUCLEAR FACTOR Y, SUBUNIT A2)
ath-miR169 h,i,j,k,l,m,n	AT1G72830	HAP2C, ATHAP2C, NF-YA3 NF-YA3 (NUCLEAR FACTOR Y, SUBUNIT A3); transcription factor
ath-miR172a,b-3p	AT5G12900	unknown protein
ath-miR172a,b-3p	AT4G29430	rps15ae ribosomal protein S15A E
ath-miR211a-5p,b-5p	AT2G19590	ACO1, ATACO1 ACC oxidase 1
ath-miR399b,e	AT2G33770	UBC24, ATUBC24, PHO2 PHO2 (PHOSPHATE 2); ubiquitin-protein ligase

Predicted Arabidopsis genes differentially expressed (DE) in 3-d-post-inoculation (dpi) giant cells and 3–7-dpi galls induced by *Meloidogyne javanica* and *M. incognita* in *Arabidopsis thaliana* (Jammes *et al.*, 2005; Barcala *et al.*, 2010) as putative targets of the differentially expressed miRNAs described within the manuscript. Red, induced, and green, repressed in galls.

Those sRNAs associated with DNA, rasiRNAs (most of them 24-nt long; Axtell, 2013), from control and gall samples were mapped in the five Arabidopsis chromosomes. Their distribution was concentrated in the same areas (mostly centromeric) for controls and galls, although the total rasiRNAs number was much higher in galls than in controls (Fig. 7), similarly to that occurring for the gall-exclusive and control root-exclusive rasiRNAs (Fig. S3). From the 27 groups or families of repetitive sequences identified in the six libraries, 16 were induced in galls with respect to the controls and only two were less abundant (Table 4; $P < 0.05$). All of these results suggest that the abundance or 24-nt sRNAs (most probably also rasiRNAs), constitutes a gall hallmark as well.

Discussion

Under the generic name of small RNA (sRNA), a plethora of diverse RNA molecules of 20–30 nt that have emerged as major regulators in plants still have little-known roles in plant–nematode interactions. The only data concerning root–knot nematode (RKN)–plant interactions were the role of miRNAs in systemic changes caused by the infection (Zhao *et al.*, 2015). Here we describe for the first time the sRNA population differential expression (DE) in RKN-induced galls compared to uninfected root segments. Our results indicate that the abundance of 24-nt sRNAs (most probably rasiRNAs) constitutes a gall hallmark, at least at early infection stages (Fig. 2). We also describe the first functional role during a plant–nematode interaction for a tasiRNA, TAS3a, regulated by miR390a in galls. This regulatory module is highly conserved from the moss *Physcomitrella patens*

(Allen *et al.*, 2005) to higher plants (Axtell *et al.*, 2006). Our study was performed with three independent biological replicates for galls and for control roots. Accordingly, we had a high validation rate for the abundance tendencies of miRNAs and their putative gene targets by independent techniques based on q-PCR and microarrays (Fig. 3). Galls are pseudo-organs formed by the expansion of giant cells (GCs), the proliferation of the neighboring vascular tissues and the hypertrophy of cortical cells in response to the nematode infection (Escobar *et al.*, 2015). Therefore, sRNAs detected in this study by high-throughput sequencing could be originated from GCs and from any of these cell types.

We obtained sequences of 21 and 24-nt as the most abundant in the six libraries (Fig. 2). This is consistent with the scarce existing data on massive sRNAs sequencing in cyst–nematode feeding sites (Hewezi *et al.*, 2008, 2012; Li *et al.*, 2012). We found differences in sRNA length distribution between galls and control roots: 21-nt sRNAs (the length of most plant miRNAs; Axtell, 2013) were more abundant in uninfected root libraries than in gall libraries, whereas 24-nt sRNAs, (the typical length of rasiRNAs; Axtell, 2013) were amply more abundant in galls. Only 11 miRNAs were upregulated in galls, whereas 51 miRNAs were downregulated. These data strongly suggest a general down-regulation of miRNAs in early-developing galls, as reported for 4-d-post-inoculation (dpi)-syncytia (Hewezi *et al.*, 2008). Most downregulated miRNAs in galls are induced or have a confirmed role in other stress conditions or nutritional statuses (Guleria *et al.*, 2011), with the exception of two miRNAs from the same family (miR156i, h), probably related to hypoxia (Guleria *et al.*, 2011), which were induced in galls (Table 1). Although hypoxia

Table 4 Repeat associated small interfering RNA (rasiRNAs) in *Meloidogyne javanica* galls and control root libraries

Type		Unique Reads						FC	P value
		G1	G2	G3	R1	R2	R3		
DNA/En-Spm	Antisense	12 324	10 919	11 389	5193	5921	6432	1.9	0.001
	Sense	16 168	14 660	15 019	5722	6334	7043	2.3	0.001
DNA/Harbinger	Antisense	3068	2672	2842	1893	1964	2194	1.4	0.007
	Sense	3942	3446	3639	2089	2194	2404	1.6	0.003
DNA/hAT-Ac	Antisense	7114	6390	7022	4393	4373	4826	1.5	0.001
	Sense	6072	5246	5578	3138	3284	3491	1.6	0.002
DNA/MuDR	Antisense	62 474	57 081	58 722	39 919	42 600	46 227	1.3	0.001
	Sense	65 456	60 306	62 294	40 907	43 668	47 507	1.4	0.000
DNA/TcMar-Mariner	Antisense	278	227	261	278	301	317	−1.2	0.038
	Sense	25 452	23 074	24 568	15 505	16 393	17 736	1.4	0.001
LINE/L1	Antisense	40 596	36 065	39 289	22 187	23 629	25 230	1.6	0.001
	Sense	1167	1027	1105	780	854	911	1.3	0.008
LTR/Copia	Antisense	28 689	25 912	27 391	14 858	15 972	17 389	1.6	0.001
	Sense	38 615	35 199	36 448	17 196	18 791	20 583	1.9	0.000
LTR/Gypsy	Antisense	54 906	49 407	51 941	24 441	26 914	29 642	1.9	0.001
	Sense	69 655	63 209	65 910	32 429	36 191	39 162	1.8	0.000
Other/Composite	Antisense	712	699	676	554	545	676	1.1	0.011
	Sense	22 238	20 305	20 770	16 397	16 985	18 957	1.2	0.007
RC/Helitron	Antisense	6329	5392	6131	4247	4018	4593	1.3	0.011
	Sense	1459	1396	1328	478	554	645	2.4	0.000
rRNA	Antisense	1066	1037	967	439	536	576	1.9	0.000
	Sense	6815	6131	5993	2650	2811	3123	2.1	0.003
Satellite	Antisense	4410	4211	4066	2096	2112	2375	1.9	0.000
	Sense	3010	2581	3136	3269	3416	3697	−1.2	0.032
SINE/tRNA	Antisense	210	202	237	139	132	142	1.5	0.007
	Sense								

Number of unique reads in the six libraries are listed. Fold change (FC) and statistical significance (*P*-value) for the differentially expressed groups of repeat associated small interfering RNA (rasiRNAs).

inside galls has not been confirmed, indirect evidences come from the activation in tobacco GCs induced by *Meloidogyne javanica* of a hemoglobin promoter that responds to low oxygen tension (Ehsanpour & Jones, 1996). Additionally, other hypoxia-related genes were also induced in 3-dpi galls (Barcala *et al.*, 2010; Cabello *et al.*, 2014), for example, a gene encoding a class I non-symbiotic leghemoglobin with high oxygen affinity (At2g16060; Hunt *et al.*, 2002), an alcohol dehydrogenase-coding gene (At1g77120), and *SUS1/SUS4*, upregulated in roots under hypoxia (Bieniawska *et al.*, 2007).

Examples of stress-induced miRNAs that were repressed in galls include members of the miR169 family induced under drought (Li *et al.*, 2008; Zhao *et al.*, 2011), low temperature (Zhou *et al.*, 2007; Lee *et al.*, 2010), high soil salinity (Zhao *et al.*, 2009), N deficiency (Zhao *et al.*, 2010) and UV-B radiation (Zhou *et al.*, 2007). Further examples are miR391 and miR399, which are prominently induced upon phosphate starvation and involved in inorganic phosphate homeostasis maintenance (Lundmark *et al.*, 2010; Guleria *et al.*, 2011), and miR780, induced under N starvation (Liang *et al.*, 2012). Their repression might indicate that N and P status are maintained in galls, probably being a basic requirement to sustain nematode feeding. This is also in accordance with the global downregulation of stress-related genes in early-developing GCs and galls in Arabidopsis and tomato (Jammes *et al.*, 2005; Schaff *et al.*, 2007; Caillaud *et al.*, 2008; Barcala *et al.*, 2010; Portillo *et al.*, 2013).

Other gall-repressed miRNAs are associated with developmental processes, for example, *MIR166/165* genes, which regulates shoot apical meristem and floral development in parallel to the WUSCHEL-CLAVATA pathway (Jung & Park, 2007), or miR156 (a, b, c, d, e, f, j) that regulates the juvenile-to-adult transition (Wu *et al.*, 2009). In this respect, cyst nematodes secrete peptides similar to CLAVATA-LIKE ELEMENTS (CLE-like) plant ligands, which have a role during syncytia formation (Replogle *et al.*, 2011, 2013). Other CLE-like peptides, such as 16D10 from RKNs, interact with transcription factors such as SCARECROW, a key regulator of radial patterning in the Arabidopsis root (Levesque *et al.*, 2006). Thus, the repression of these miRNAs in galls might be related to developmental processes contributing to maintain a balance between cell proliferation and differentiation in the complex gall structure (Table 1).

Although the reasons and functional consequences of massive miRNA repression in galls is currently far from being understood, downregulation of several miRNAs has been reported in several plant species during interactions with different pathogens such as fungi, viruses or bacteria (Balmer & Mauch-Mani, 2013). In Arabidopsis infected with *Heterodera schachtii*, miR396 downregulation and subsequent *GRF1/GRF3* induction are necessary for correct syncytia initiation (Hewezi *et al.*, 2012). In mammals, general miRNA-mediated gene repression contributes to cancer by promoting transposable element (TE) expression that benefits the evolving tumor by leading to genomic instability

(Shalgi *et al.*, 2010). Accordingly, we have identified several miRNAs as being downregulated in early-developing galls that may target TEs in the Arabidopsis genome (Tables S2, S3).

The most abundant miRNA induced in 3-dpi galls is miR390 (Table 1). miR390a and TAS3-derived tasiRNAs define a pathway that regulates leaf patterning establishing leaf polarity and controls lateral root growth by repressing the *ARF* family members *ARF2*, *ARF3* and *ARF4* (Hunter *et al.*, 2006; Nogueira *et al.*, 2007; Marin *et al.*, 2010). Previously, a molecular link between lateral root formation and galls was demonstrated by the crucial role during gall formation of *LBD16*, an essential gene for lateral root development which is regulated by auxins (Cabrera *et al.*, 2014a), similarly to miR390a. Here we describe another regulatory network shared by galls and lateral roots, based on the regulatory action of miR390 on TAS3-derived tasiRNAs (Figs 4–6). The expression patterns of miR390a and TAS3a promoters overlapped in galls, particularly in the vascular tissue and GCs (Fig. 4). Loss-of-function lines showed increased resistance to *M. javanica* and their galls were smaller than in control plants (Fig. 5). Remarkably, TAS3-derived tasiRNAs were active in galls, as proven by the fact that an *ARF3::GUS*-based sensor line showed no signal in wild-type galls, whereas a line carrying an *ARF3* mutation resistant to TAS3-derived tasiRNAs showed GUS activity restricted to the gall centre, including GCs (Fig. 6). These results concur with our former data from microarrays, where *ARF4*, another demonstrated target of TAS3-derived tasiRNAs in lateral roots (Marin *et al.*, 2010), was repressed in 3-dpi GCs (Barcala *et al.*, 2010). Thus, we identify for the first time in the Arabidopsis–RKN interaction a complex regulatory module that involves two sRNA types: an miRNA highly abundant in galls, miR390, and the TAS3-derived tasiRNAs, actively functioning in both galls and GCs. Although, Arabidopsis is not a natural host for RKNs, the transcriptomes of early GCs induced by *M. javanica* in Arabidopsis and tomato roots showed a high similarity (Portillo *et al.*, 2013). Furthermore, genes such as the peroxidase *TPX1*, downregulated in Arabidopsis GCs at 3 dpi as well as its corresponding ortholog in tomato (Barcala *et al.*, 2010; Portillo *et al.*, 2013) with a demonstrably crucial role for GCs/gall formation in tomato, provide another specific example. These findings validate holistic approaches in the Arabidopsis genetic model for simplicity, and launch the potential to transfer this knowledge to crop plants.

Galls showed a higher abundance in 24-nt sRNA sequences than control roots, most of them being gall-exclusive or upregulated (Fig. S2). Most of these sequences match repetitive sequences in the genome, like TEs (Table 4; Fig. 7). More than 16 out of 26 transposon families predicted to produce the tasiRNAs identified in uninfected roots and galls were over-represented in galls (Table 4). Among them, hAT and PIF/Harbinger families are highly enriched in euchromatic regions in maize and have been related to heterosis (He *et al.*, 2013). tasiRNAs play a pivotal role in gene silencing through the RNA-dependent DNA methylation (RdDM) pathway (Weiberg *et al.*, 2014). In RdDM, the RNA polymerase IV/RDR2/DCL3/AGO4/6/9 module induces DNA methylation through 24 nt sRNAs, which is maintained by MET1 and CMT3. In

accordance, *MET1* is upregulated in Arabidopsis GCs (Barcala *et al.*, 2010) and a chromomethylase involved in DNA methylation (Lindroth *et al.*, 2001) is induced in tomato GCs (Portillo *et al.*, 2013). Moreover, previous microarray results showed a drastic repression of gene expression in GCs as compared to control roots. This tendency was conserved in early-developing GCs (3 dpi) and galls of Arabidopsis and tomato (Jammes *et al.*, 2005; Barcala *et al.*, 2010; Portillo *et al.*, 2013). Thus, in this context, it is possible that epigenetic processes regulated by 24-nt sRNAs mediate gene repression during early stages of GC differentiation from their vascular precursors. A similar abundance of 24-nt sRNAs was found in a *Verticillium*-sensitive cultivar of *Gossypium hirsutum*, infected with *Verticillium dahlia*, a soil-borne fungal pathogen (Yang *et al.*, 2013). Suppression of the RdDM silencing pathway increased Arabidopsis resistance to *Pseudomonas syringae* (Downe *et al.*, 2012), suggesting that this pathway is important for bacterial infection.

In soybean, DNA hypermethylation has been observed in cyst nematode-resistant lines with multiple Rhg1 copies (Cook *et al.*, 2014). Strikingly, tasiRNA transcripts can also generate 24-nt sRNAs in plants (Allen *et al.*, 2005; Khraiweh *et al.*, 2010). These induce cytosine methylation at tasiRNA-generating loci (Wu *et al.*, 2012), similarly to 21-nt secondary siRNAs generated by DCL4 that participate in post-transcriptional silencing of exogenous targets through AGO1 (Cuperus *et al.*, 2010). In this respect, a recent differential methylation study (methylooma) of Arabidopsis DNA extracted from soybean roots infected with *H. schachtii* (Rambani *et al.*, 2015) showed DNA methylation changes during the compatible interaction that impact a large number of protein coding genes locally in the syncytium and systemically. A significant portion of the differentially methylated genes was among genes with differential expression in the soybean syncytium. These results point to a novel role of syncytia-induced DNA methylation in regulating gene expression changes during parasitism (Rambani *et al.*, 2015).

In conclusion, a plethora of sRNAs is present in early-developing galls. Among them, some miRNAs will contribute to the gene silencing observed in GCs via target mRNA degradation, translation inhibition, or by regulation of ta-siRNAs, such as miR390-TAS3. The scenario gets more complex, as one of the gall molecular signatures is the high abundance of 24-nt sRNAs known to mediate epigenetic regulation of gene expression through chromatin remodeling. Future research will elucidate these sRNA-mediated mechanisms that probably orchestrate the developmental processes participating in gall and GC differentiation.

Acknowledgements

This work was supported by the Spanish Government (AGL2013-48787 to C.E. and PCIN-2013-053 to C.F.) and by the Castilla-la Mancha Government (PEII-2014-020-P to C.F.). J.C. was supported by a fellowship from the Ministry of Education, Spain. C.M. was supported by a PhD grant from INRA-SPE Dpt and the Conseil Régional Provence-Alpes-Côte d'Azur (PACA). B.F. was supported by the French Government

(National Research Agency, ANR) through the 'Investments for the Future' LabEx SIGNALIFE (ANR-11-LABX-0028-01).

Author contributions

J.C., C.F. and C.E. planned and designed the research. J.C., M.B., A.G., A.R.-M., C.M. and A.M. performed experiments and analysed data. J.C., V.R.-F, S.J.-P, B.F, C.F and C.E. wrote the manuscript. All authors made changes to the initial manuscript and revised the final version.

References

- Allen E, Xie Z, Gustafson AM, Carrington JC. 2005. microRNA-directed phasing during trans-acting siRNA biogenesis in plants. *Cell* 121: 207–221.
- Aukerman MJ, Sakai H. 2003. Regulation of flowering time and floral organ identity by a microRNA and its APETALA2-like target genes. *Plant Cell* 15: 2730–2741.
- Axtell MJ. 2013. Classification and comparison of small RNAs from plants. *Annual Review of Plant Biology* 64: 137–159.
- Axtell MJ, Jan C, Rajagopalan R, Bartel DP. 2006. A two-hit trigger for siRNA biogenesis in plants. *Cell* 127: 565–577.
- Balmer D, Mauch-Mani B. 2013. Small yet mighty – microRNAs in plant-microbe interactions. *Microna* 2: 72–79.
- Barcala M, Garcia A, Cabrera J, Casson S, Lindsey K, Favery B, Garcia-Casado G, Solano R, Fenoll C, Escobar C. 2010. Early transcriptomic events in microdissected Arabidopsis nematode-induced giant cells. *Plant Journal* 61: 698–712.
- Bar-Or C, Kapulnik Y, Koltai H. 2005. A broad characterization of the transcriptional profile of the compatible tomato response to the plant parasitic root knot nematode *Meloidogyne javanica*. *European Journal of Plant Pathology* 111: 181–192.
- Bieniaszka Z, Paul Barratt DH, Garlick AP, Thole V, Kruger NJ, Martin C, Zrenner R, Smith AM. 2007. Analysis of the sucrose synthase gene family in Arabidopsis. *Plant Journal* 49: 810–828.
- Bohlmann H. 2015. Introductory chapter on the basic biology of cyst nematodes. In: Escobar C, Fenoll C, eds. *Advances in botanical research: plant nematode interactions*, vol. 73. Oxford, UK: Elsevier, 33–59.
- Bologna NG, Voinnet O. 2014. The diversity, biogenesis, and activities of endogenous silencing small RNAs in Arabidopsis. *Annual Review of Plant Biology* 65: 473–503.
- Bonnet E, Wuyts J, Rouzé P, Van de Peer Y. 2004. Evidence that microRNA precursors, unlike other non-coding RNAs, have lower folding free energies than random sequences. *Bioinformatics* 20: 2911–2917.
- Cabello S, Lorenz C, Crespo S, Cabrera J, Ludwig R, Escobar C, Hofmann J. 2014. Altered sucrose synthase and invertase expression affects the local and systemic sugar metabolism of nematode-infected *Arabidopsis thaliana* plants. *Journal of Experimental Botany* 65: 201–212.
- Cabrera J, Bustos R, Favery B, Fenoll C, Escobar C. 2014a. NEMATIC: a simple and versatile tool for the *in silico* analysis of plant-nematode interactions. *Molecular Plant Pathology* 15: 627–636.
- Cabrera J, Diaz-Manzano FE, Sanchez M, Rosso MN, Melillo T, Goh T, Fukaki H, Cabello S, Hofmann J, Fenoll C *et al.* 2014b. A role for *LATERAL ORGAN BOUNDARIES-DOMAIN 16* during the interaction Arabidopsis-*Meloidogyne* spp. provides a molecular link between lateral root and root-knot nematode feeding site development. *New Phytologist* 203: 632–645.
- Caillaud MC, Dubreuil G, Quentin M, Perfus-Barbeoch L, Lecomte P, de Almeida Engler J, Abad P, Rosso MN, Favery B. 2008. Root-knot nematodes manipulate plant cell functions during a compatible interaction. *Journal of Plant Physiology* 165: 104–113.
- Cook DE, Bayless AM, Wang K, Guo X, Song Q, Jiang J, Bent AF. 2014. Distinct copy number, coding sequence, and locus methylation patterns underlie Rhg1-mediated soybean resistance to soybean cyst nematode. *Plant Physiology* 165: 630–647.
- Cuperus JT, Montgomery TA, Fahlgren N, Burke RT, Townsend T, Sullivan CM, Carrington JC. 2010. Identification of MIR390a precursor processing-defective mutants in Arabidopsis by direct genome sequencing. *Proceedings of the National Academy of Sciences, USA* 107: 466–471.
- Dai X, Zhao PX. 2011. psRNATarget: a plant small RNA target analysis server. *Nucleic Acids Research* 39: W155–W159.
- Downen RH, Pelizzola M, Schmitz RJ, Lister R, Downen JM, Nery JR, Dixon JE, Ecker JR. 2012. Widespread dynamic DNA methylation in response to biotic stress. *Proceedings of the National Academy of Sciences, USA* 109: E2183–E2191.
- Ehsanpour AA, Jones MG. 1996. Glucuronidase expression in transgenic tobacco roots with a parasponia promoter on infection with *Meloidogyne javanica*. *Journal of Nematology* 28: 407–413.
- Escobar C, Barcala M, Cabrera J, Fenoll C. 2015. Overview of root-knot nematodes and giant cells. In: Escobar C, Fenoll C, eds. *Advances in botanical research: plant nematode interactions*, vol. 73. Oxford, UK: Elsevier, 1–32.
- Escobar C, Sigal B, Mitchum M. 2011. Transcriptomic and proteomic analysis of the plant response to nematode infection. In: Jones J, Gheysen G, Fenoll C, eds. *Genomics and molecular genetics of plant-nematode interactions*. Dordrecht, the Netherlands: Springer, 157–176.
- Frenquelli M, Muzio M, Scielzo C, Fazi C, Scarfò L, Rossi C, Ferrari G, Ghia P, Caligaris-Cappio F. 2010. MicroRNA and proliferation control in chronic lymphocytic leukemia: functional relationship between miR-221/222 cluster and p27. *Blood* 115: 3949–3959.
- Ghildiyal M, Zamore PD. 2009. Small silencing RNAs: an expanding universe. *Nature Reviews Genetics* 10: 94–108.
- Guleria P, Mahajan M, Bhardwaj J, Yadav SK. 2011. Plant small RNAs: biogenesis, mode of action and their roles in abiotic stresses. *Genomics Proteomics Bioinformatics* 9: 183–199.
- Harfouche L, Haichar Fel Z, Achouak W. 2015. Small regulatory RNAs and the fine-tuning of plant-bacteria interactions. *New Phytologist* 206: 98–106.
- He G, Chen B, Wang X, Li X, Li J, He H, Yang M, Lu L, Qi Y, Wang X *et al.* 2013. Conservation and divergence of transcriptomic and epigenomic variation in maize hybrids. *Genome Biology* 14: R57.
- Hewezi T, Baum TJ. 2015. Gene silencing in nematode feeding sites. In: Escobar C, Fenoll C, eds. *Advances in botanical research: plant nematode interactions*, vol. 73. Oxford, UK: Elsevier, 221–239.
- Hewezi T, Howe P, Maier TR, Baum TJ. 2008. Arabidopsis small RNAs and their targets during cyst nematode parasitism. *Molecular Plant-Microbe Interactions* 21: 1622–1634.
- Hewezi T, Maier TR, Nettleton D, Baum TJ. 2012. The Arabidopsis microRNA396-GRF1/GRF3 regulatory module acts as a developmental regulator in the reprogramming of root cells during cyst nematode infection. *Plant Physiology* 159: 321–335.
- Hunt PW, Klok EJ, Trevaskis B, Watts RA, Ellis MH, Peacock WJ, Dennis ES. 2002. Increased level of hemoglobin 1 enhances survival of hypoxic stress and promotes early growth in *Arabidopsis thaliana*. *Proceedings of the National Academy of Sciences, USA* 99: 17 197–17 202.
- Hunter C, Willmann MR, Wu G, Yoshikawa M, de la Luz Gutierrez-Nava M, Poethig SR. 2006. Trans-acting siRNA-mediated repression of ETTIN and ARF4 regulates heteroblasty in Arabidopsis. *Development* 133: 2973–2981.
- Jagga Z, Gupta D. 2014. Supervised learning classification models for prediction of plant virus encoded RNA silencing suppressors. *PLoS ONE* 9: e97446.
- Jammes F, Lecomte P, de Almeida-Engler J, Bitton F, Martin-Magniette ML, Renou JP, Abad P, Favery B. 2005. Genome-wide expression profiling of the host response to root-knot nematode infection in Arabidopsis. *Plant Journal* 44: 447–458.
- Jung J-H, Park C-M. 2007. MIR166/165 genes exhibit dynamic expression patterns in regulating shoot apical meristem and floral development in Arabidopsis. *Planta* 225: 1327–1338.
- Kanno T, Yoshikawa M, Habu Y. 2013. Locus-specific requirements of DDR complexes for gene-body methylation of TAS genes in *Arabidopsis thaliana*. *Plant Molecular Biology Reporter* 31: 1048–1052.
- Khraiwesh B, Arif MA, el Seum GI, Ossowski S, Weigel D, Reski R, Frank W. 2010. Transcriptional control of gene expression by microRNAs. *Cell* 140: 111–122.
- Klink VP, Hosseini P, Matsye P, Alkharouf NW, Matthews BF. 2009. A gene expression analysis of syncytia laser microdissected from the roots of the *Glycine*

- max* (soybean) genotype PI 548402 (Peking) undergoing a resistant reaction after infection by *Heterodera glycines* (soybean cyst nematode). *Plant Molecular Biology* 71: 525–567.
- Klink VP, Hosseini P, Matsye PD, Alkharouf NW, Matthews BF. 2010. Syncytium gene expression in *Glycine max* (PI 88788) roots undergoing a resistant reaction to the parasitic nematode *Heterodera glycines*. *Plant Physiology and Biochemistry* 48: 176–193.
- Lee H, Yoo SJ, Lee JH, Kim W, Yoo SK, Fitzgerald H, Carrington JC, Ahn JH. 2010. Genetic framework for flowering-time regulation by ambient temperature-responsive miRNAs in *Arabidopsis*. *Nucleic Acids Research* 38: 3081–3093.
- Levesque MP, Vernoux T, Busch W, Cui H, Wang JY, Blilou I, Hassan H, Nakajima K, Matsumoto N, Lohmann JU *et al.* 2006. Whole-genome analysis of the SHORT-ROOT developmental pathway in *Arabidopsis*. *PLoS Biology* 4: e143.
- Li W-X, Oono Y, Zhu J, He X-J, Wu J-M, Iida K, Lu X-Y, Cui X, Jin H, Zhu J-K. 2008. The *Arabidopsis* NFYA5 transcription factor is regulated transcriptionally and posttranscriptionally to promote drought resistance. *Plant Cell Online* 20: 2238–2251.
- Li X, Wang X, Zhang S, Liu D, Duan Y, Dong W. 2012. Identification of soybean microRNAs involved in soybean cyst nematode infection by deep sequencing. *PLoS ONE* 7: e39650.
- Liang G, He H, Yu D. 2012. Identification of nitrogen starvation-responsive microRNAs in *Arabidopsis thaliana*. *PLoS ONE* 7: e48951.
- Lindroth AM, Cao X, Jackson JP, Zilberman D, McCallum CM, Henikoff S, Jacobsen SE. 2001. Requirement of CHROMOMETHYLASE3 for maintenance of CpXpG methylation. *Science* 292: 2077–2080.
- Lundmark M, Korner CJ, Nielsen TH. 2010. Global analysis of microRNA in *Arabidopsis* in response to phosphate starvation as studied by locked nucleic acid-based microarrays. *Physiologia Plantarum* 140: 57–68.
- Marin E, Jouanet V, Herz A, Lokerse AS, Weijers D, Vaucheret H, Nussaume L, Crespi MD, Maizel A. 2010. miR390, *Arabidopsis* TAS3 tasiRNAs, and their AUXIN RESPONSE FACTOR targets define an autoregulatory network quantitatively regulating lateral root growth. *Plant Cell* 22: 1104–1117.
- Mitkowski NA, Abawi GS. 2003. Root-knot nematodes. *Plant Health Instructor* 2011: doi: 10.1094/PHI-I-2003-0917-0.
- Montgomery TA, Howell MD, Cuperus JT, Li D, Hansen JE, Alexander AL, Chapman EJ, Fahlgren N, Allen E, Carrington JC. 2008. Specificity of ARGONAUTE7-miR390 interaction and dual functionality in TAS3 trans-acting siRNA formation. *Cell* 133: 128–141.
- Navarro L, Dunoyer P, Jay F, Arnold B, Dharmasiri N, Estelle M, Voinnet O, Jones JD. 2006. A plant miRNA contributes to antibacterial resistance by repressing auxin signaling. *Science* 312: 436–439.
- Nogueira FT, Madi S, Chitwood DH, Juarez MT, Timmermans MC. 2007. Two small regulatory RNAs establish opposing fates of a developmental axis. *Genes & Development* 21: 750–755.
- Nuthikattu S, McCue AD, Panda K, Fultz D, DeFraia C, Thomas EN, Slotkin RK. 2013. The initiation of epigenetic silencing of active transposable elements is triggered by RDR6 and 21–22 nucleotide small interfering RNAs. *Plant Physiology* 162: 116–131.
- Portillo M, Cabrera J, Lindsey K, Topping J, Andres MF, Emiliozzi M, Oliveros JC, Garcia-Casado G, Solano R, Koltai H *et al.* 2013. Distinct and conserved transcriptomic changes during nematode-induced giant cell development in tomato compared with *Arabidopsis*: a functional role for gene repression. *New Phytologist* 197: 1276–1290.
- Portillo M, Lindsey K, Casson S, Garcia-Casado G, Solano R, Fenoll C, Escobar C. 2009. Isolation of RNA from laser-capture-microdissected giant cells at early differentiation stages suitable for differential transcriptome analysis. *Molecular Plant Pathology* 10: 523–535.
- R Development Core Team 2008. *R: A language and environment for statistical computing*. Vienna Austria: R Foundation for Statistical Computing. URL <http://www.R-project.org> [accessed 01 September 2015].
- Rambani A, Rice JH, Liu J, Lane T, Ranjan P, Mazarei M, Pantalone V, Stewart CN Jr, Staton M, Hewezi T. 2015. The methylome of soybean roots during the compatible interaction with the soybean cyst nematode. *Plant Physiology* 168: 1364–1377.
- Replogle A, Wang J, Bleckmann A, Hussey RS, Baum TJ, Sawa S, Davis EL, Wang X, Simon R, Mitchum MG. 2011. Nematode CLE signaling in *Arabidopsis* requires CLAVATA2 and CORYNE. *Plant Journal* 65: 430–440.
- Replogle A, Wang J, Paolillo V, Smeda J, Kinoshita A, Durbak A, Tax FE, Wang X, Sawa S, Mitchum MG. 2013. Synergistic interaction of CLAVATA1, CLAVATA2, and RECEPTOR-LIKE PROTEIN KINASE 2 in cyst nematode parasitism of *Arabidopsis*. *Molecular Plant–Microbe Interactions* 26: 87–96.
- Schaff JE, Nielsen DM, Smith CP, Scholl EH, Bird DM. 2007. Comprehensive transcriptome profiling in tomato reveals a role for glycosyltransferase in Mi-mediated nematode resistance. *Plant Physiology* 144: 1079–1092.
- Shalgi R, Pilpel Y, Oren M. 2010. Repression of transposable-elements – a microRNA anti-cancer defense mechanism? *Trends in Genetics* 26: 253–259.
- Smant G, Jones J. 2011. Suppression of plant defences by nematodes. In: Jones J, Gheysen G, Fenoll C, eds. *Genomics and molecular genetics of plant–nematode interactions*. Dordrecht, the Netherlands: Springer, 273–286.
- Sunkar R, Li Y-F, Jagadeeswaran G. 2012. Functions of microRNAs in plant stress responses. *Trends in Plant Science* 17: 196–203.
- Thimm O, Blasing O, Gibon Y, Nagel A, Meyer S, Kruger P, Selbig J, Muller LA, Rhee SY, Stitt M. 2004. MAPMAN: a user-driven tool to display genomics data sets onto diagrams of metabolic pathways and other biological processes. *Plant Journal* 37: 914–939.
- Weiberg A, Wang M, Bellinger M, Jin H. 2014. Small RNAs: a new paradigm in plant–microbe interactions. *Annual Review of Phytopathology* 52: 495–516.
- Wu G, Park MY, Conway SR, Wang JW, Weigel D, Poethig RS. 2009. The sequential action of miR156 and miR172 regulates developmental timing in *Arabidopsis*. *Cell* 138: 750–759.
- Wu G, Poethig RS. 2006. Temporal regulation of shoot development in *Arabidopsis thaliana* by Mir156 and its target SPL3. *Development* 133: 3539–3547.
- Wu L, Mao L, Qi Y. 2012. Roles of dicer-like and argonaute proteins in TAS-derived small interfering RNA-triggered DNA methylation. *Plant Physiology* 160: 990–999.
- Xu M, Li Y, Zhang Q, Xu T, Qiu L, Fan Y, Wang L. 2014. Novel miRNA and phasiRNA biogenesis networks in soybean roots from two sister lines that are resistant and susceptible to SCN race 4. *PLoS ONE* 9: e110051.
- Yang X, Wang L, Yuan D, Lindsey K, Zhang X. 2013. Small RNA and degradome sequencing reveal complex miRNA regulation during cotton somatic embryogenesis. *Journal of Experimental Botany* 64: 1521–1536.
- Zhang Z, Yu J, Li D, Zhang Z, Liu F, Zhou X, Wang T, Ling Y, Su Z. 2010. PMRD: plant microRNA database. *Nucleic Acids Research* 38: D806–D813.
- Zhao M, Ding H, Zhu J-K, Zhang F, Li W-X. 2011. Involvement of miR169 in the nitrogen-starvation responses in *Arabidopsis*. *New Phytologist* 190: 906–915.
- Zhao B, Ge L, Liang R, Li W, Ruan K, Lin H, Jin Y. 2009. Members of miR-169 family are induced by high salinity and transiently inhibit the NF-YA transcription factor. *BMC Molecular Biology* 10: 29–29.
- Zhao W, Li Z, Fan J, Hu C, Yang R, Qi X, Chen H, Zhao F, Wang S. 2015. Identification of jasmonic acid-associated microRNAs and characterization of the regulatory roles of the miR319/TCP4 module under root-knot nematode stress in tomato. *Journal of Experimental Botany* 66: 4653–4667.
- Zhao CZ, Xia H, Frazier TP, Yao YY, Bi YP, Li AQ, Li MJ, Li CS, Zhang BH, Wang XJ. 2010. Deep sequencing identifies novel and conserved microRNAs in peanuts (*Arachis hypogaea* L.). *BMC Plant Biology* 10: 3.
- Zhou X, Wang G, Zhang W. 2007. UV-B responsive microRNA genes in *Arabidopsis thaliana*. *Molecular Systems Biology* 3: 103–103.

Supporting Information

Additional supporting information may be found in the online version of this article.

Fig. S1 Expression pattern of *pMIR390a::GUS* and *pTAS3a::GUS* in noninfected plant roots and in roots infected with *M. incognita*.

Fig. S2 Pie charts indicating the number of 24 nt sequences that are exclusive, up-or downregulated in gall and control root libraries.

Fig. S3 Distribution of repeat associated small interfering RNA (rasiRNAs) exclusive of galls and roots among the five Arabidopsis chromosomes.

Table S1 Sequence of primers used for the analysis of miRNA target genes by real time q-PCR

Table S2 Number of reads found in the six libraries generated of known miRNAs found in miRBase for Arabidopsis

Table S3 Putative target genes identified for all the differentially expressed known miRNAs

Table S4 Putative target genes identified for the differentially expressed novel miRNAs

Please note: Wiley Blackwell are not responsible for the content or functionality of any supporting information supplied by the authors. Any queries (other than missing material) should be directed to the *New Phytologist* Central Office.



About New Phytologist

- *New Phytologist* is an electronic (online-only) journal owned by the New Phytologist Trust, a **not-for-profit organization** dedicated to the promotion of plant science, facilitating projects from symposia to free access for our Tansley reviews.
- Regular papers, Letters, Research reviews, Rapid reports and both Modelling/Theory and Methods papers are encouraged. We are committed to rapid processing, from online submission through to publication 'as ready' via *Early View* – our average time to decision is <27 days. There are **no page or colour charges** and a PDF version will be provided for each article.
- The journal is available online at Wiley Online Library. Visit **www.newphytologist.com** to search the articles and register for table of contents email alerts.
- If you have any questions, do get in touch with Central Office (np-centraloffice@lancaster.ac.uk) or, if it is more convenient, our USA Office (np-usaoffice@lancaster.ac.uk)
- For submission instructions, subscription and all the latest information visit **www.newphytologist.com**